Dynamic Response of Long Optical-Cavity Laser Diode for *Ka*-Band Communication Satellites

Afshin S. Daryoush, *Senior Member, IEEE,* Kenji Sato, *Member, IEEE,*
Kohji Horikawa, *Member, IEEE,* and Hiroyo Ogawa, *Member, IEEE*

***Abstract*— This paper presents the performance of a novel Fabry–Perot (FP) laser diode. The laser is composed of a long gain section, and a multiple-quantum-well (MQW) electro-absorption (E/A) modulator. The laser diode is mode locked using the integrated E/A modulator at 19.3 GHz. Sub-carrier data signals at S-band and a frequency reference of 19.3 GHz are simultaneously distributed using modulation of the gain and E/A sections of the laser, respectively. This paper also compares performance of this laser diode at various operation points in terms of pulsewidth, pulse-to-pulse coherency, phase-noise degradation of the frequency reference, and two-tone spurious-free dynamic range. Implication of this laser's performance as an optical transmitter is also evaluated for a fiber-optic (FO) distribution network in Ka-band phased-array antennas for satellite communications.**

***Index Terms*— Communication satellites, laser diodes, mode-locking, optical beamforming networks, pulse coherency.**

I. Introduction

FUTURE communication satellites are designed to operate at frequencies of Ka-band using active phase-array antennas. The challenge of distributing Ka-band signals from central processing unit (CPU) to the active transmit/receive (T/R) modules of a phased array could be overcome by a fiber-optic (FO) distribution link. Both directly and externally modulated FO links have been employed to demonstrate distribution of the analog signals [1]; however, because of the reliability, size, and cost, the directly modulated FO distribution networks are more attractive in satellite-communication applications. Unfortunately, the physical limitations of present laser structures have restricted practical system applications of the directly modulated FO links to the frequencies of a few gigahertz.

Various methods, such as mode coupling [2], subharmonic injection locking of a laser with external cavity [3], and mode locking [4], have been demonstrated to increase the highest carrier frequency of the narrow-bandwidth directly modulated FO links. Alternative system architecture, labeled *T/R level data mixing*, is proposed to separately distribute the Ka-band carrier and the sub-carrier data signals [5], [6], as depicted in Fig. 1 for a satellite down-link at Ka-band. The sub-carrier data is up-converted to Ka-band by phase and frequency coherent self-oscillating mixers (SOM's) [7]. Each SOM is phase and frequency locked, using injection-locked phase-locked loop (ILPLL) technique [8]. Using the *T/R level data mixing* technique a higher spurious-free dynamic range (SFDR) is obtained at Ka-band over the conventional *CPU level data-mixing* method [9]. Distribution of the reference and sub-carrier data signals should be performed in a single optical transmitter (E/O), while maintaining the highest SFDR and power-consumption efficiency (cf. Fig. 1).

This paper presents experimental demonstration of such an optical transmitter to be used in conjunction with the *T/R level data mixing* architecture. More specifically, a long Fabry–Perot (FP) laser diode structure, integrated with an electro-absorption (EA) modulator is employed as an E/O to distribute both frequency reference of 19.3 GHz and sub-carrier data signals at S-band. In Section II, structure of this novel laser diode is discussed and the static performance of the fabricated laser are presented. In Section III, the dynamic performance of the laser diode is presented. Experimental results that demonstrate mode locking of a large number of the longitudinal modes of the FP laser are first presented followed by experiments evaluating the spectral purity of a 19.3-GHz mode-locked pulses. Finally, result of spurious-free dynamic-range measurements at S-band is presented for this laser diode. Section IV evaluates the impact of the mode-locking techniques in the overall system's performance, which is then discussed for future Ka-band communication satellites.

II. Device Structure

Active mode locking is an attractive technique in digital FO links where the pulse train is synchronized with an electrical reference (clock signal). Active mode locking is considered as a viable method to generate high optical power at frequencies beyond the semiconductor laser bandwidth. Although the preliminary experiments have been reported on lasers with external cavities, a lot of efforts are recently directed toward monolithically integrated mode-locked lasers. It is now recognized that by monolithic integration of gain section, passive waveguide, and modulator-section, stable and reliable mode locking is obtained. Active, passive, and hybrid mode locking by monolithic lasers have been reported [10]–[15]. Our design approach is to monolithically integrate an FP laser with an EA modulator. This device is primarily developed for short

Manuscript received December 12, 1996; revised April 30, 1997.

A. S. Daryoush was with NTT Wireless Systems Laboratories, NTT Opto-Electronics Laboratories, Atsugi-shi, Yokosuka-shi, Kanagawa, Japan. He is now with the ECE Department, Drexel University, Philadelphia, PA 19104 USA.

K. Sato is with NTT Opto-Electronics Laboratories, Atsugi-shi, Yokosuka-shi, Kanagawa, Japan.

K. Horikawa and H. Ogawa are with NTT Wireless Systems Laboratories, Yokosuka-shi, Kanagawa, Japan.

Publisher Item Identifier S 0018-9480(97)06023-7.

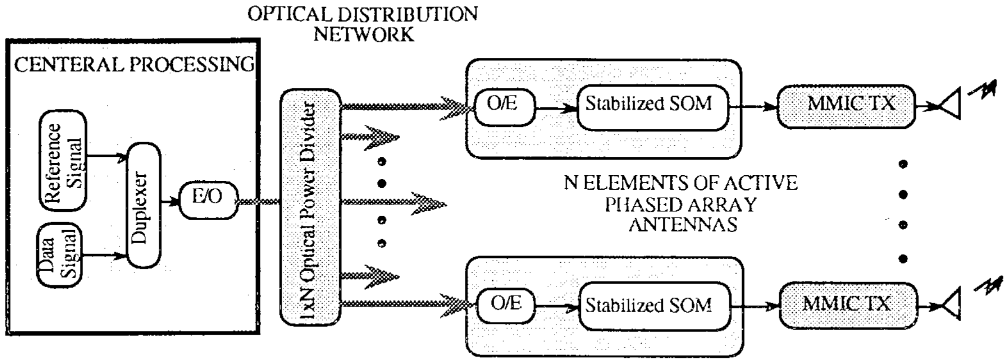

Fig. 1. Conceptual representation of the optical distribution of a frequency reference (19.3 GHz) and sub-carrier data signals (S-band) to N elements of a Ka-band phase-array antennas. The reference signal is used to synchronize 19.3-GHz local oscillators in the SOM. The received sub-carrier data signal is up-converted by the stabilized SOM to generate an RF signal at Ka-band. (E/O and O/E are optical transmitter and receiver modules. MMIC TX represents a MMIC-based transmitter module.)

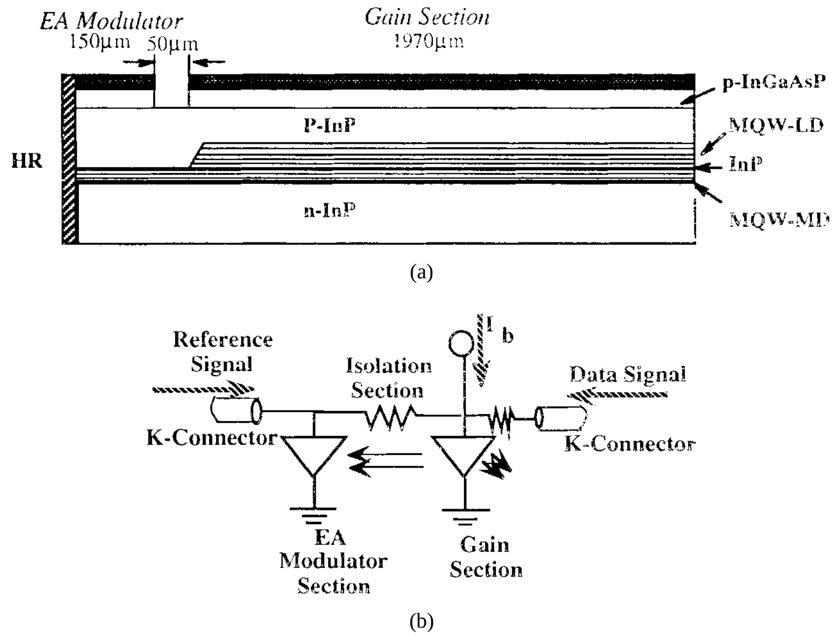

Fig. 2. (a) Conceptual device structure of a long FP laser that is integrated with an E/A modulator. (b) Schematic diagram of the long FP laser diode integrated with an EA modulator.

pulse generation, since EA modulator has a wide modulation bandwidth.

Fig. 2(a) shows a schematic drawing of the monolithic laser with an integrated EA modulator. Stacked structure consisting of two multiple-quantum-well (MQW) layers, a MQW for laser diode (MQW-LD), and a MQW for EA modulator (MQW-MD) are employed. The details of this structure and the fabrication process are described in [16]. The FP cavity length for our experiment is approximately cleaved for a length of 2170 μm. This total length is composed of a gain section, high-resistivity separation region, and modulator section. The resistance between the gain and the EA-modulator sections is over 20 kΩ. The facet of the modulator section is coated with high reflective film, whereas the gain section's facet is cleaved.

The laser is mounted in a high-frequency (HF) package. The schematic diagram of the long FP laser with an integrated EA modulator is shown in Fig. 2(b). RF inputs to the gain and EA-modulator sections are through the K connectors' transition to microstrip lines. The 50-Ω microstrip lines are realized on alumina substrates. The gain section is resistively matched to 50 Ω using a series thin-film resistor. The EA modulator is left unmatched.

A threshold of 42 and 73.5 mA is measured for the EA-modulator's bias voltage of $V_m = -1.0$ V and $V_m = -4.5$ V, respectively. On the other hand, the differential efficiency of 0.09 mW/mA and 0.04 mW/mA is measured above threshold for the EA reverse-bias voltages of 1.0 V and 4.5 V, respectively. The lower differential efficiency of the laser at the EA-modulator's dc bias of $V_m = -4.5$ V is attributed to a higher loss in the EA modulator and the gain saturation in the gain section.

III. Experimental Results

Standard experimental setup is employed to characterize dynamic behavior of this laser. The laser output is collimated to a single-mode optical fiber using the polarizing collimator.

Integrated with this collimator is an optical isolator with isolation of ≥40 dB. The fiber output is split in two paths using a 3-dB optical coupler. Each path is connected through a meter-long single-mode optical fiber to various instruments.

The optical characteristics of the laser are monitored on various test equipment. The optical spectra and coherency of the laser are monitored on an optical-spectrum analyzer (Advantest Q8347). A streak camera is also employed to monitor the mode-locked short optical pulses in time domain. The microwave-frequency characteristics of the laser are monitored using an HP70004A system, and an integrated broad-band optical receiver (HP70810B) combined with a high dynamic-range RF analyzer (HP70908A). This calibrated measurements of laser-frequency response, relative-intensity noise (RIN), and mode-partition noise are easily converted to a relative electrical signal by multiplying the displayed results in decibels by a factor of two.

The mode-locking experiments are conducted by providing a dc bias and microwave signal to the EA-modulator section of the monolithically integrated laser. The frequency-stabilized output of an HP83640A is amplified by an HP83017A power amplifier and then used as a calibrated source for the mode-locking experiments. Both dc and RF signals are provided to the EA-modulator by the Bias-T. The two-tone intermodulation distortion (IMD) experiments are conducted by providing the S-band signals to the RF input port of the gain section. Two microwave sweep oscillators (HP8625A) are coupled through a 90° hybrid to generate a calibrated output over the S-band; however, only the experimental results of two tones of 2.200 and 2.205 GHz are reported here.

A. Mode Locking

Throughout the reported experiments, the laser diode's temperature is actively stabilized to 20 °C. The gain section of the laser diode is forward biased at different bias currents and the EA section is reverse biased by different voltage levels. The natural-frequency response of the laser is monitored on the HP70004A system. At first, the EA modulator is not modulated by the frequency reference of 19.3 GHz. The frequency response of the laser is measured at various laser bias currents, ranging from $I_b = 80$ mA up to $I_b = 150$ mA for bias voltage of $V_m = 0$ V. A resonance peak is observed, which is associated with the longitudinal-mode separation in the long FP laser. The longitudinal-mode separation is calculated as $\Delta f = c/2nL \approx 19.3$ GHz, where $c = 300$ mm. Gigahertz is speed of light in free space, $n \approx 3.5$ is the index of refraction of the waveguide, and $L \approx 2.17$ mm is the length of the FP cavity. This resonant frequency has a frequency tuning sensitivity of ≈1 MHz/mA.

Comparison between the dynamic performances of this long-cavity laser diode at $I_b = 100$ and $I_b = 140$ mA when the EA modulator is reverse biased at 4.5 V is depicted in Fig. 3. A large number of spurious signals appears in the frequency response, as seen in Fig. 3(a) for $P_m = 0$ mW. These spurious peaks are strongly present up to the laser bias current of $I_b \approx 130$ mA. At the bias current of 100 mA, it appears that the resonance peak is now shifted to a frequency

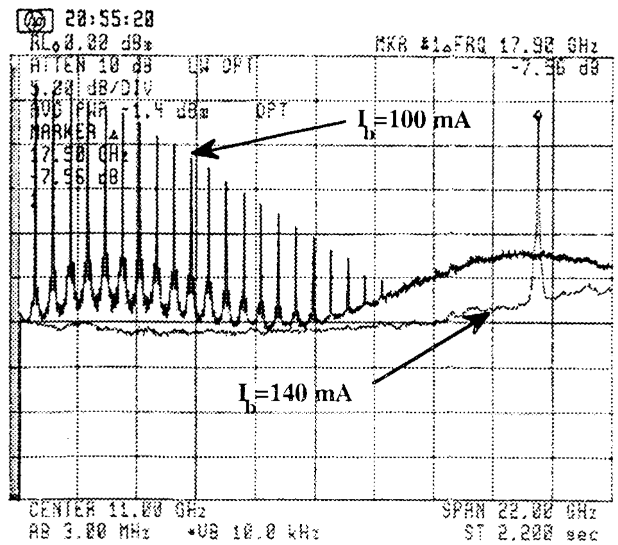

(a)

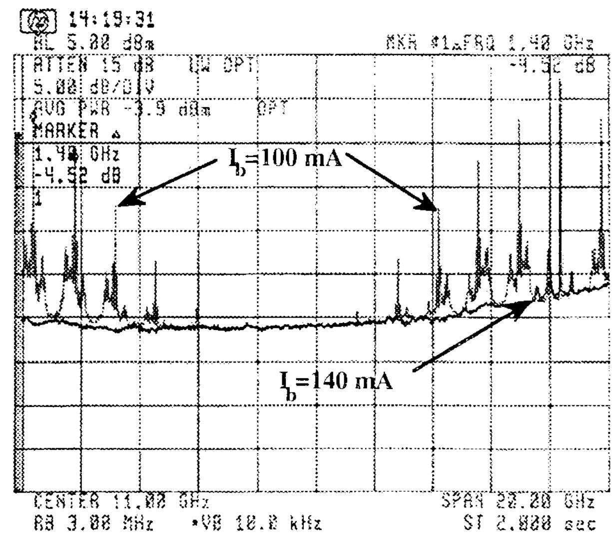

(b)

Fig. 3. Frequency response of the novel laser at gain-section dc-bias current levels of $I_b = 100$ and $I_b = 140$ mA at EA-modulator dc bias of $V_m = -4.5$ V. (a) Free-running at $P_m = 0$ mW. (b) Mode locked at $P_m = +15$ dBm and $f_m \approx 19.3$ GHz.

as low as 18 GHz. In addition to the resonance peak at ≈18 GHz, self-modulation of ≈600 MHz is also observed. The resonance peak shifts to a higher frequency as the bias current increases. As the laser bias current is increased to 140 mA, the frequency response is now much cleaner and the strong self-modulation, which is seen at 100 mA, is not present anymore. In fact, a distinctive resonant peak at ≈19.3 GHz appears. This resonance peak is not very stable, and is not useful as a reference signal in microwave applications unless it is frequency and phase are stabilized.

As the EA-modulator section is modulated by a synthesized-frequency reference signal of $f_m = 19.300$ GHz at $P_m \geq -5$ dBm, a resonance peak at 19.300 GHz now starts to appear, even for the $I_b = 100$ mA. The self-modulation shifts to a higher frequency of 750 MHz when the EA section is modulated by an RF power level of $P_m \approx -5$ dBm. The

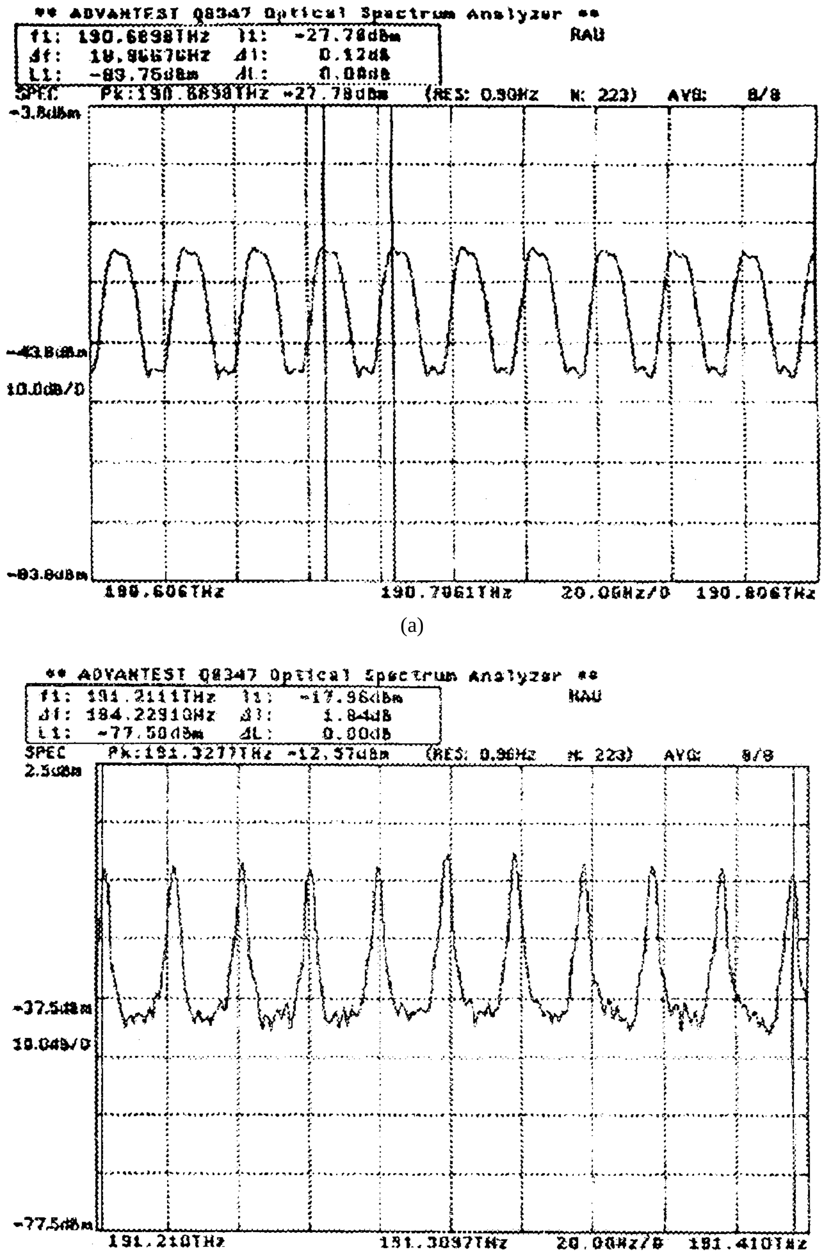

(a)

(b)

Fig. 4. Optical spectra of the mode-locked optical pulse trains. (a) $I_b = 100$ mA and $V_m = -4.5$ V. (b) $I_b = 140$ mA and $V_m = -1.0$ V.

strong self-modulation signals are present for bias currents up to $I_b \leq 120$ mA and the self-modulation frequencies changes from 600 MHz up to 1.38 GHz. The resonance modulation component becomes far more dominant at the $P_m \geq +15$ dBm for $I_b = 100$ mA, as shown in Fig. 3(b). These self-modulation frequencies are attributed to the relaxation oscillation frequency competing with the mode-locking process. The self-modulation could be avoided by changing the modulating frequency to the natural oscillation frequency or by increasing the modulation power beyond +15 dBm. In fact, a distinctive resonance peak without any spurious self-modulation is attained for $I_b = 100$ mA, $V_m = -4.5$ V, $f_m = 19.2$ GHz, and $P_m \approx +18$ dBm. However, this frequency is different from the desired operation frequency of 19.3 GHz.

Even though the self-modulation is absent for $I_b = 140$ mA, a closer observation of the spectra at 19.3 GHz indicates modulation sidebands of ≈ 200 MHz. These small sidebands are associated with the mode-partition noise and are also observed at the $I_b = 100$ mA. For a fixed modulating power $P_m = +15$ dBm, as the EA-modulator's bias voltage is increased from $V_m = -4.5$ to $V_m = 0$ V, the distinctive resonant now peak easily at all bias currents above threshold. The resonance peak appears without experiencing any self-modulation. To observe a spurious-free resonance peak, the required laser-bias current shifts to a higher level as the EA-modulator's reverse-bias voltage increases. It appears that for achieving a high amplitude signal at 19.3 GHz, free of any spurious self-modulation, the best EA-modulator's bias point for this device is at $V_m = -1.0$ V. Note that the benefit of

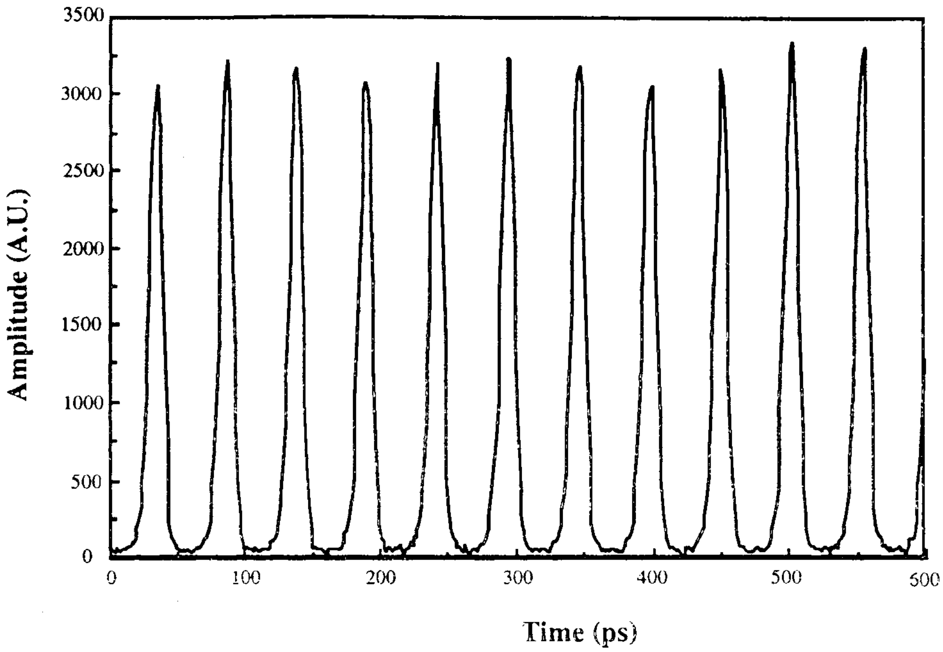

(a)

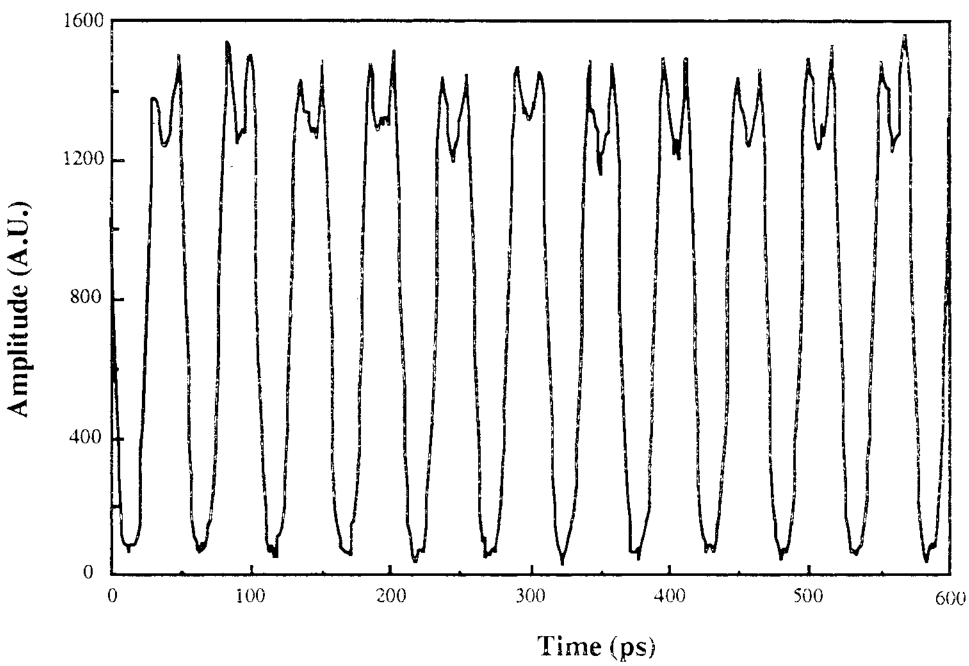

(b)

Fig. 5. Streak camera traces of the mode-locked pulses for two different EA-modulator's bias voltage at gain-section dc bias of $I_b = 140$ mA, EA-modulator's modulating $P_m = +15$ dBm, $f_m = 19.3$ GHz. (a) $V_m = -4.5$ V. (b) $V_m = -1.0$ V.

modulating the EA section is that the resonant peak is now stabilized and a mode-locked train of pulses occurs.

The measured mode-locked optical spectra at $f_m = 19.3$ GHz and $P_m = +15$ dBm is shown in Fig. 4, as the resonance peak is now stabilized. Fig. 4(a) renders the measured mode-locked pulses for the $I_b = 100$ mA and $V_m = -4.5$ V, whereas Fig. 4(b) depicts the measured mode-locked pulse trains for $I_b = 140$ mA and $V_m = -1.0$ V. Note that the pulse-to-pulse separation is calculated to be ≈ 19.3 GHz. Time-domain representation of the optical-pulse trains are measured for $I_b = 140$ mA using a streak camera, as depicted in Fig. 5. The measured pulsewidth of 11 ps, shown in Fig. 5(a), is for the operating point of $V_m = -4.5$ V, whereas the mode-locked pulsewidth of 29 ps is measured for $V_m = -1.0$ V [cf. Fig. 5(b)]. Note that for both cases, the laser is mode locked. For $I_b = 100$ mA and operating at $f_m = 19.2$ GHz and $P_m = +18$ dBm (i.e., under the best conditions to avoid the ≈ 1-GHz relaxation oscillation related spurious self-modulation) a shorter pulsewidth (≈ 7 ps) is also obtained for $V_m = -4.5$ V as opposed to $V_m = -2.5$ V (≈ 14 ps) operating points.

TABLE I
MEASURED COHERENCY OF MODE-LOCKED PULSE TRAINS T, AND SINGLE-PULSE DISPERSION TIME τ. THE SINGLE-PULSE DISPERSION τ IS THE TIME SPREAD FROM AN IDEAL IMPULSE BEHAVIOR FOR THE SINGLE MODE-LOCKED PULSE UNDER THE CONDITION THAT THE PULSE COHERENCY IS HIGHER THAN 10%. THE PULSE TRAIN COHERENCY TIME T IS DEFINED AS THE TOTAL TIME SEPARATION BETWEEN TWO MODE-LOCKED PULSES THAT ARE 80% COHERENT. THE MODE-LOCKING FREQUENCY IS AT $f_m = 19.300$ GHz AND $V_m = -1.0$V

I_b (mA)	P_M (mW)	Pulse Train Coherency Time T (psec)	Single Pulse Dispersion τ (psec)
140	0	619	9.6
140	30	928	7.5

TABLE II
MEASURED SINGLE-PULSE COHERENCY OF MODE-LOCKED PULSE TRAINS AT $I_b = 140$ mA, $P_m = 15$ dBm, AND $f_m = 19.300$ GHz AT DIFFERENT EA-MODULATOR'S BIAS VOLTAGE

V_m (V)	Single-Pulse Dispersion Time τ (psec)	Pulse Train Coherency Time T (psec)
-1.0	9.6	928
-1.5	5.5	331
-3.0	3.4	176
-4.5	3.1	165

TABLE III
MEASURED CLOSE-IN TO THE CARRIER PHASE NOISE AT 19.300 000 GHz AND THE FM NOISE DEGRADATION OF THE MODE-LOCKED PULSES WITH RESPECT TO THE REFERENCE SIGNAL AT TWO OFFSET CARRIER FREQUENCIES OF $\Omega = 100$ AND $\Omega = 500$ Hz

		£(Ω) (dBc/Hz)		Δ (dB)	
I_b (mA)	V_m (V)	Ω=100Hz	Ω=500Hz	Ω=100Hz	Ω=500Hz
100	-4.5	-70	-81	10	2
140	-1.0	-75	-82	5	1

To verify the streak camera results at 140 mA, coherency measurements are also conducted using the optical-spectrum analyzer. The concept of coherency measurements is based on the optical version of an electrical correlator, in which a lightwave is homodyned by a delayed version of itself. For a single pulse, the correlation time is directly related to the pulsewidth and coherency of the pulse. Since in the case of a mode-locked laser a single laser pulse is coherent far longer than its pulsewidth, then the coherency distance is a measure of the optical pulsewidth. Therefore, the coherency measurements are analyzed over a narrow range of $\pm$ 2.9 mm to measure 10% coherency pulsewidth τ, with a time resolution of better than 0.5 ps. On the other hand, by looking at the coherency over a maximum coherency measurement range of $\pm$165 mm one can extract coherency of a single pulse to a reference pulse. Parameter T is selected as a figure of merit and related to a total time for pulses to remain coherent better than 80% of the time.

Table I compares the coherency time of 19.3-GHz resonance peak for the mode-locked case versus the unlocked case. As expected, superior performance is measured for the mode-locked case. Results of the coherency measurements as a function of the EA-modulator bias levels are summarized in Table II for mode-locked pulses at $I_b = 140$ mA. It is clear that the shortest pulsewidth are truly obtained at $V_m = -4.5$ V as the streak camera results suggest. Table II also depicts comparison of T parameters, where the longest pulse-to-pulse coherency time is achieved for $V_m = -1.0$ V. It is interesting to note that the short pulse does not necessarily relate to a higher pulse-to-pulse coherency.

Since the pulse-to-pulse coherency is an approximate measure of the spectral purity of the modulated frequency reference at 19.3 GHz, modulator bias of $V_m = -1.0$ V is, therefore, selected as the best operating point, even though the pulsewidth is not the narrowest. Measurement of the pulse-to-pulse coherency T for the $I_b = 100$ mA, $V_m = -4.5$ V, and modulating frequency of 19.3 GHz corresponds to a value of 100 ps. This behavior is expected since the spurious oscillation degrades the overall coherency. The close-in to carrier phase-noise measurements are also conducted as a measure of the mode-locked pulse-to-pulse coherency. Comparison of the close-in to carrier phase noise at offset frequencies as low as 100 Hz are presented in Table III. These results compare performance of the best case of $I_b = 140$ mA and $V_m = -1.0$ V to the worst case of $I_b = 100$ mA and $V_m = -4.5$ V. The results indicate that the FM-noise degradation as high as 10 dB is measured for $I_b = 100$ mA and $V_m = -4.5$ V as compared to only 5 dB for $I_b = 140$ mA and $V_m = -1.0$ V. These results could be explained from the A.M./P.M. conversion as result of the higher RIN noise at $I_b = 100$ mA [17]. The measured close-in to carrier phase noise for the mode-locked laser at $V_m = -4.5$ V at the offset frequencies of $\Omega = 100$ Hz and $\Omega = 500$ Hz are identical to the results of $V_m = -1.0$ V for the same laser current of $I_b = 140$ mA.

B. Sub-Carrier Data Modulation

In the *T/R level data mixing* architecture, shown in Fig. 1, the overall system dynamic range is dominated by the SFDR of the FO link at the sub-carrier data signal frequency. SFDR is calculated based on the input third-order intercept point, noise figure, and gain of the system. In the directly modulated FO link, the third-order intercept point and noise figure are dominated by the laser diode characteristics [1]. Since the RIN of the laser diode dictates the noise floor level of the system, RIN measurements are conducted at the various bias conditions. Table IV summarizes the measured RIN for the mode-locked laser biased at 140 mA. As the results of Table IV suggest, the lowest RIN level is obtained at $V_m \approx -1.0$ V. Therefore, from the coherency and noise floor level the best noise performance is attained at $V_m \approx -1.0$ V.

TABLE IV
MEASURED RELATIVE-INTENSITY NOISE OF THE MODE-LOCKED LASER AT 2.200 GHz AS A FUNCTION OF THE EA-MODULATOR'S BIAS VOLTAGE OF V_m. MODE-LOCKING IS AT $I_b = 140$ mA, $P_m = +15$ dBm, AND $f_m = 19.3$ GHz

V_m (V)	-0.5	-1.5	-2.5	-3.5	-4.5
RIN (dB/Hz)	-139.6	-139.4	-137.3	-130.3	-130.2

TABLE V
COMPARISON OF (IP3), THE RIN, AT INFORMATION FREQUENCY OF 2.200 GHz, AND THE CALCULATED SFDR FOR THE BIAS CURRENTS OF 100 AND 140 mA AT THE BIAS VOLTAGE OF $V_m = -1$V APPLIED TO THE EA SECTION OF THE LASER WITH A LONG OPTICAL CAVITY

I_b (mA)	P_m (mW)	IP3 (dBm)	RIN (dB/Hz)	SFDR (dB.Hz$^{2/3}$)
100	0	+15	-134	88
140	0	+22	-140	96
140	30	+21	-139	95

In addition to the RIN measurements, IMD measurements are also performed to determine the nonlinearity of this laser diode. The IMD measurements are conducted to evaluate performance of the mode-locked laser for sub-carrier data transmission. Two tones of $f_1 = 2.200$ and $f_2 = 2.205$ GHz are injected to the gain section of the laser diode as opposed to the EA section. Fundamental tones, f_1 and f_2, and the third IMD's of $2f_1 - f_2 = 2.195$ and $2f_2 - f_1 = 2.210$ GHz are measured on the HP70004A system. The measured results are converted to the relative electrical signals by multiplying the measured optical power in decibels by a factor of 2. A higher third-order intercept point (IP3) is measured when the laser is not mode locked and operated at a higher bias current. Results of IP3 and RIN measurements are employed to calculate the SFDR, as shown in Table V for $V_m = -1.0$ V. It is evident that even though mode locking causes small reduction in the SFDR, its impact is not as severe as improper operation point.

IV. DISCUSSIONS AND CONCLUSIONS

The presented experimental results are indicative of great potential for this novel laser structure as an optical transmitter for optically controlled phase-array antennas. In particular, simultaneous distribution of frequency reference at 19.3 GHz and sub-carrier data signals at S-band are demonstrated as part of the *T/R level data mixing* architecture, which could be, in-turn, up-converted to Ka-band communication satellite frequency band using an SOM at 19.3 GHz. Further improvement in the achieved SFDR can be made by use of reactive matching of the optical transmitter as opposed to the resistive matching of the laser diode [1]. In fact, SFDR of 101 dB·Hz$^{2/3}$ and 103 dB·Hz$^{2/3}$ are measured for the mode-locked ($P_m = 30$ mW) and free-running ($P_m = 0$ mW) operation of a reactively matched version of this optical transmitter which operates at $I_b = 140$ mA and $V_m = -1.0$ V, respectively. Since the SFDR of the sub-carrier data FO link will determine the overall SFDR of the modulated carrier at Ka-band [7], the measured SFDR of 101 dB·Hz$^{2/3}$ is already higher than the 96 dB·Hz$^{2/3}$, which is the best reported performance of any directly modulated FO link performance above 12 GHz [1].

The streak camera measurement of short optical pulses indicates that a shorter pulsewidth is achieved when the mode-locking power causes a full voltage swing between low- and high-loss regions [19]. Therefore, for short-pulse operation, the EA modulator should be operated in the reverse-bias operating points corresponding to the high-loss portion of the loss versus voltage curve [20]. However, from a modulation efficiency standpoint, it is best to operate at the linear portion of the loss versus voltage curve. Finally, from the spectra purity of the frequency reference (i.e., pulse-to-pulse coherency of mode-locked pulses) it appears that the best operation point to be at is the low-loss region. However, even though far away from the carrier ($\Omega > 10$ kHz), the reference and the mode-locked signals appears to have the same spectral purity, close-in to the carrier ($\Omega < 1$ kHz) measurements of single sideband (SSB) phase noise reveals a phase-noise degradation difference as high as 5 dB. In fact, in a low-sensitivity measurement system typically experienced when a spectrum-analyzer is used for the SSB phase-noise measurements of not a super-clean reference signal, it is the residual phase noise of the mode-locked signal to clearly account for the phase noise contribution of the mode-locked laser to the phase noise degradation of the super-clean reference signal [17].

REFERENCES

[1] A. S. Daryoush, E. Ackerman, N. Samant, S. Wanuga, and D. Kasemset, "Interfaces for high-speed fiberoptic links: Analysis and experiment," *IEEE Trans. Microwave Theory Tech.*, vol. 39. pp. 2031–2044, Dec. 1991.

[2] K. Lau, "Short-pulse and high-frequency signal generation in semiconductor lasers," *J. Lighwave Technol.*, vol. 7, pp. 400–419, Feb. 1989.

[3] T. D. Ni, X. Zhang, and A. S. Daryoush, "Dynamic range of semiconductor laser in the presence of external cavity," *IEEE Microwave Guided Wave Lett.*, vol. 4, pp. 68–70, Mar. 1994.

[4] S. Levy, R. Nagarajan, A. Mar, P. Humphrey, and J. E. Bowers, "Fiber-optic PSK subcarrier transmission at 35 GHz using a resonantly enhanced semiconductor laser," *Electron. Lett.*, vol. 28, no. 22, pp. 2103–2104, Oct. 1992.

[5] A. S. Daryoush, "Optical synchronization of millimeter-wave oscillators for distributed millimeter-wave systems," *IEEE Trans. Microwave Theory Tech.*, vol. 38, pp. 1371–1373, May 1990.

[6] A. S. Daryoush, E. Ackerman, R. Saedi, R. Kunath, and K. Shalkhauser, "High-speed fiber optic links for distribution of satellite traffic," *IEEE Trans. Microwave Theory Tech.*, vol. 38, pp. 510–517, May 1990.

[7] X. Zhou and A. S. Daryoush, "An efficient self-oscillating mixer for communications" *IEEE Trans. Microwave Theory Tech.*, vol. 42, pp. 1858–1862, Oct. 1994.

[8] X. Zhou, X. Zhang, and A. S. Daryoush, "A new approach for a phase controlled self-oscillating mixer," *IEEE Trans. Microwave Theory Tech.*, vol. 45, pp. 1858–1862, Feb. 1997.

[9] R. Saedi *et al.*, "Comparison of CPU level data mixing to T/R level data mixing architectures in optically controlled phased arrays," *Inter. Microwave Symp.*, Atlanta GA, June 1993.

[10] R. S. Tucker, U. Koren, G. Raybon, C. A. Burrus, B. I. Miller, T. L. Koch, G. Eisenstein, and A. Shahar, "40 GHz active mode locking in a 1.5 μm monolithic extended-cavity laser," *Electron. Lett.*, vol. 25, no. 10, pp. 621–622, May 1989.

[11] P. A. Morton, J. E. Bowers, L. A. Koszi, M. Soler, J. Lopata, and D. P. Wilt, "Monolithic hybrid mode-locked 1.3 μm semiconductor lasers," *Appl. Phys. Lett.*, vol. 56, no. 2, pp. 111–113, Jan. 1990.

[12] Y. K. Chen, M. C. Wu, T. Tanbun-Ek, R. A. Logan, and M. A. Chin, “Subpicosecond monolithic colliding-pulse mode-locked multiple quantum well lasers,” *Appl. Phys. Lett.*, vol. 58, no. 12, pp. 1253–1255, Mar. 1991.

[13] P. B. Hansen, G. Raybon, U. Koren, P. P. Iannone, B. I. Miller, G. M. Young, M. A. Newkirk, and C. A. Burrus, “InGaAsP monolithic extended-cavity lasers with integrated saturable absorbers for active, passive, and hybrid mode locking at 8.6 GHz,” *Appl. Phys. Lett.*, vol. 62, no. 13, pp. 1445–1447, Mar. 1993.

[14] S. Arahira, Y. Matsui, T. Kunii, S. Oshiba, and Y. Ogawa, “Optical short pulse generation at high repetition rate over 80 GHz from a monolithic passively modelocked DBR laser diode,” *Electron. Lett.*, vol. 29, no. 11, pp. 1013–1014, May 1993.

[15] K. Wakita, K. Sato, I. Kotaka, M. Yamamoto, and M. Asobe, “Transform-limited 7-ps optical pulse generation using a siusoidally driven InGaAsP/InGaAsP strained multiple-quantum-well DFB laser/modulator monolithically integrated light source,” *IEEE Photon. Technol. Lett.*, vol. 5, pp. 899–901, Aug. 1993.

[16] K. Sato, K. Wakita, I. Kotaka, Y. Kondo, and M. Yamamoto, “Monolithic strained-InGaAsP multiple-quantum-well lasers with integrated electroabsorption modulators for active mode locking,” *Appl. Phys. Lett.*, vol. 65, no. 1, pp. 1–4, July 1994.

[17] T. D. Ni, X. Zhang, and A. S. Daryoush, “Experimental study on close-in carrier phase noise of laser diode with coherent feedback,” *IEEE Trans. Microwave Theory Tech.*, vol. 43, pp. 2277–2283, Sept. 1995.

[18] E. Ackerman and A. S. Daryoush, “Broad-band external modulation fiber-optic links for antenna-remoting applications,” this issue, pp. 1436–1442.

[19] K. Sato, I. Kotaka, Y. Kondo, and M. Yamamoto, “Active mode locking at 50-GHz repetition frequency by half-frequency modulation of monolithic semiconductor lasers integrated with electroabsorption modulators,” *Appl. Phys. Lett.*, vol. 69, no. 18, pp. 2626–2628, Oct. 1996.

[20] K. Kawano, K. Wakita, O. Mitomi, I. Kotaka, and M. Naganuma, “Design of InGaA-InAlAs multiple-quantum-well (MQW) optical modulators,” *IEEE J. Quantum Electron.*, vol. 28, pp. 224–230, Jan. 1992.

Afshin S. Daryoush (S’84–M’86–SM’91) received the Ph.D. degree in electrical engineering from Drexel University, Philadelphia, PA, in 1986.

He then joined the faculty of Drexel University as DuPont Assistant Professor of electrical and computer engineering, and in 1990, became an Associate Professor. During the summer of 1987 and 1988, he was a Summer Faculty Fellow at NASA-Lewis Research Center, Cleveland, OH, working on analog fiber-optic links for ACTS. In the summers of 1989 and 1990, he was with the Naval Air Development Center, Warminster, PA, as an ASEE Summer Faculty Fellow working on low-power-consuming digital fiber-optic links, and was a Visiting Scholar at NTT Wireless Systems Laboratories, Yokosuka, Japan, from October 1996 to April 1997. Currently he is with the ECE Department, Drexel University. He has authored or co-authored over 150 technical publications, conducted research in microwave photonics, and lectured frequently at workshops and international symposia.

Dr. Daryoush is a member of Sigma Xi and serves as the Drexel University chapter chairman in 1997–1998. He has served as guest editor for *The Journal of Franklin Institute* and *Microwave & Lightwave Technology Letters* and the Philadelphia Joint Chapter of the IEEE Antennas and Propagation and Microwave Theory and Techniques Societies in various capacities, including chairman from 1991 to 1993. He is a member of the MTT-3 Technical Committee and IEEE Editorial Press. He has been awarded four U.S. patents and one international patent. He is the recipient of the Microwave Prize at the 16th European Microwave Conference, Dublin, Ireland, and has also received the Best Paper Award at the 1986 International Microwave Symposium, Baltimore, MD.

Kenji Sato (M’95) received the B.S., M.S., and Ph.D. degrees from Nagoya University, Nagoya, Japan, in 1978, 1980, and 1992, respectively.

In 1980, he joined NTT Electrical Communications Laboratories. He is currently a Senior Research Engineer with the NTT Opto-Electronics Laboratories, Atsugi-shi, Kanagawa, Japan. His current interests include long-wavelength lasers, modulators, and optical short pulse sources.

Dr. Sato is a member of IEEE LAser and Electro-Optic Society, the Physical Society of Japan, the Japan Society of Applied Physics, and the Institute of Electronics, Information, and Communication Engineers.

Kohji Horikawa (M’93) received the B.E. degree in electrical engineering from the Tokyo Institute of Technology, Tokyo, Japan, in 1984.

In 1984, he joined Yokosuka Electrical Communication Laboratories, NTT, Yokosuka, Japan. He is currently a Senior Research Engineer at NTT Wireless Systems Laboratories, Yokosuka-shi, Kanagawa, Japan. He has been engaged in research and development of satellite onboard transponders. Since 1993, he has been researching optical/microwave interaction systems and photonic beam-forming networks for microwave active phase-array antennas.

Mr. Horikawa is a member of the American Institute of Aeronautics and Astronautics (AIAA), International Society for Optical Engineering (SPIE), and Institute of Electronics, Information and Communication Engineers (IEICE) of Japan.

Hiroyo Ogawa (M’84) received the B.S., M.S., and Dr. Eng. degrees in electrical engineering from Hokkaido University, Sapporo, Japan, in 1974, 1976, and 1983, respectively.

In 1976, he joined the Yokosuka Electrical Communication Laboratories, Nippon Telegraph and Telephone Public Corporation, Yokosuka, Japan. He has been engaged in research on microwave and millimeter-wave integrated circuits, monolithic integrated circuits, and development of subscriber radio systems. From 1985 to 1986, he was a Post-Doctoral Research Associate at the University of Texas at Austin, on leave from NTT. From 1987 to 1988, he was engaged in design of the subscriber radio equipment of the Network System Development Center of NTT. From 1990 to 1992, he was engaged in the research of optical/microwave monolithic integrated circuits and fiber optic links for personal communication systems at ATR Optical and Radio Communication Research Laboratories. Since 1993, he has been researching microwave and millimeter-wave signal-processing techniques for communication satellites at NTT Wireless Systems Laboratories, Yokosuka-shi, Kanagawa, Japan.

Dr. Ogawa is a member of the Institute of Electronics, Information and Communication Engineers (IEICE) of Japan. He serves on the IEEE Microwave Theory and Techniques-S Symposium Technical Committee, is a member of the Microwave Theory and Techniques Technical Committee (MTT-3), and an associate editor of the Editorial Committee of IEICE Transactions on Electronics since 1990. He also served on Microwave Theory and Techniques-Tokyo Chapter as a Secretary/Treasurer from 1991 to 1992.